

Realistic search for doubly charged bileptons at linear e^-e^- collider energies

S. Ata \ddot{g} ^{*} and K.O. Ozansoy[†]

Department of Physics, Faculty of Sciences, Ankara University, 06100 Tando \ddot{g} an, Ankara, Turkey

We search for doubly charged scalar bileptons via $e^-e^- \rightarrow \mu^-\mu^-$ and $e^-e^- \rightarrow e^-e^-$ processes at linear collider energies by considering initial and final state electromagnetic radiative corrections (ISR, FSR). Moreover, smeared cross section is used for finite energy resolution. We show that ISR+FSR and smearing reduce cross sections remarkably depending on the smearing parameter due to narrow decay width of bileptons. We obtain realistic discovery contours of couplings and masses for the lepton flavour conserving and violating processes.

PACS numbers: 12.15.Ji, 12.15.-y, 12.60.-i, 14.80. Cp

I. INTRODUCTION

In the minimal Standard Model (SM) the usual Higgs mechanism responsible for the electroweak symmetry breaking implies the conservation of the lepton number separately for each generation. As is well known, the current low energy phenomenology of the SM is quite consistent with all present experiments. However, there has been no experimental evidence for the existence of the SM Higgs boson. This is one of the good reasons that other symmetry breaking mechanisms and extended Higgs sectors have not been excluded in the theoretical point of view. In addition, indication for neutrino oscillations necessarily violates lepton-flavour symmetry[1]. In the theories beyond the SM doubly charged, lepton flavour changing, exotic bosons may occur. Models with extended Higgs sectors include doubly charged Higgs boson [2]. In the supersymmetric extensions, such as SO(10) SUSY GUT model, supersymmetric lepton partners induce lepton flavor violation [3]. The purpose of this paper is to study doubly charged bilepton search through resonance channel in e^-e^- scattering in some detail including electromagnetic initial+final state radiative corrections and smearing effects. Bileptons are defined as bosons carrying lepton number $L=2$ or 0 which couple to two standard model leptons but not to quarks. Bileptons appear in left-right symmetric models [4] and also in models where $SU(2)_L$ gauge group is extended to $SU(3)$ [5]. Grand unified theories, technicolor and composite models predict the existence of bileptons as well as other exotic particles [6]. Classification and interactions of bileptons are provided by several works [7] and a comprehensive review has been presented in [8] including low and high energy bounds on their couplings. Indirect constraints on the masses and couplings of doubly charged bileptons have been obtained from μ and τ physics, muonium-antimuonium conversion and Bhabha scattering experiments [9, 10, 11, 12, 13, 14]. A search for doubly charged bilepton has been performed by DELPHI collaboration at LEP [15].

General effective lagrangian describing interactions of bileptons with the standard model leptons is generated by requiring $SU(2)_L \times U(1)_Y$ invariance. We consider the lagrangian involving the bilepton couplings to leptons only for $L=2$ bileptons as follows:

$$\begin{aligned} \mathcal{L}_{L=2} = & g_1^{ij} \bar{\ell}_i^c i\sigma_2 \ell_j L_1 + \tilde{g}_1^{ij} \bar{e}_i^c e_j R \tilde{L}_1 \\ & + g_2^{ij} \bar{\ell}_i^c i\sigma_2 \gamma_\mu e_j R L_2^\mu + g_3^{ij} \bar{\ell}_i^c i\sigma_2 \bar{\sigma} \ell_j \cdot \tilde{L}_3 + h.c. \end{aligned} \quad (1)$$

In the notations we have used ℓ is the left handed $SU(2)_L$ lepton doublet and e_R is the right handed charged singlet lepton. Charge conjugate fields are defined as $\psi^c = C\bar{\psi}^T$ and $\sigma_1, \sigma_2, \sigma_3$ are the Pauli matrices. The subscript of bilepton fields $L_{1,2,3}$ and couplings $g_{1,2,3}$ denote $SU(2)_L$ singlets, doublets and triplets. We denote flavour indices by $i, j = 1, 2, 3$

Here we are interested only in doubly charged bileptons. In order to express the lagrangian in terms of individual electron, bileptons and helicity projection operators $P_{R/L} = \frac{1}{2}(1 \pm \gamma_5)$ we expand the Pauli matrices and lepton doublets and write the lagrangian as :

$$\begin{aligned} \mathcal{L}_{L=2} = & \tilde{g}_1 \tilde{L}_1^{++} \bar{e}^c P_R e + g_2 L_{2\mu}^{++} \bar{e}^c \gamma^\mu P_L e \\ & - \sqrt{2} g_3 L_3^{++} \bar{e}^c P_L e + h.c. \end{aligned} \quad (2)$$

^{*}atag@science.ankara.edu.tr

[†]oozansoy@science.ankara.edu.tr

where superscripts of bileptons stand for their electric charges and flavour indices have been skipped. When the scalar L_3 gains a vacuum expectation value it becomes a doubly charged Higgs that appears in left-right symmetric models.

e^-e^- colliders[16] are to be considered as a component of future linear e^+e^- collider programs [17]. The initial state quantum numbers of e^-e^- colliders make them suitable to probe resonances for doubly charged bileptons.

II. CROSS SECTIONS FOR $e^-e^- \rightarrow e^-e^-$ AND $e^-e^- \rightarrow \mu^-\mu^-$ RESONANT STATES

The unpolarized differential cross section for the process $e^-e^- \rightarrow e^-e^-$ including doubly charged scalar bilepton L_3^{--} exchange with lepton flavour conserving couplings is given by

$$\frac{d\sigma}{d\cos\theta} = \frac{1}{2} \left(\frac{1}{32\pi s} \right) \frac{1}{4} [|M(LL; LL)|^2 + |M(RR; RR)|^2 + |M(LR; LR)|^2 + |M(RL; RL)|^2 + |M(LR; RL)|^2 + |M(RL; LR)|^2] \quad (3)$$

where the helicity amplitudes are given in terms of mandelstam invariants s , t and u as below

$$M(LL; LL) = -2g_e^2 s \left(\frac{1}{t} + \frac{1}{u} \right) - 2C_L^2 s \left(\frac{1}{t - M_Z^2} + \frac{1}{u - M_Z^2} \right) - g_L^2 \frac{s}{s - M_L^2 + iM_L\Gamma_L} \quad (4)$$

$$M(RR; RR) = -2g_e^2 s \left(\frac{1}{t} + \frac{1}{u} \right) - 2C_R^2 s \left(\frac{1}{t - M_Z^2} + \frac{1}{u - M_Z^2} \right) \quad (5)$$

$$M(LR; LR) = -2g_e^2 \frac{u}{t} + 2C_L C_R \frac{u}{t - M_Z^2} \quad (6)$$

$$M(RL; RL) = M(LR; LR) \quad (7)$$

$$M(LR; RL) = -2g_e^2 \frac{t}{u} - 2C_L C_R \frac{t}{u - M_Z^2} \quad (8)$$

$$M(RL; LR) = M(LR; RL) \quad (9)$$

In the above expressions we denote bilepton-lepton-lepton coupling by g_L where subscript L indicates the bilepton. M_L and $\Gamma_L = g_L^2 M_L / (16\pi)$ are scalar bilepton mass and decay width into leptons, respectively. In this work, we consider that doubly charged bileptons can decay only to leptons. The mandelstam invariant s is defined as the square of total energy of incoming particles in the center of mass system (c.m.) and other variables t and u can be written in terms of angle between incoming and outgoing leptons in c.m. system

$$t = -\frac{s}{2}(1 - \cos\theta), \quad u = -\frac{s}{2}(1 + \cos\theta) \quad (10)$$

The couplings C_L and C_R can be connected to the electromagnetic coupling parameter $g_e^2 = 4\pi\alpha_{em}$ and Weinberg angle θ_W

$$C_L = \frac{g_z}{2} (C_V + C_A), \quad C_R = \frac{g_z}{2} (C_V - C_A) \quad (11)$$

$$C_V = 2\sin^2\theta_W - \frac{1}{2}, \quad C_A = -\frac{1}{2} \quad \text{for } e, \mu, \tau \quad (12)$$

$$g_z = \frac{g_e}{\sin\theta_W \cos\theta_W} \quad (13)$$

In the case of the process $e^-e^- \rightarrow \mu^-\mu^-$ only flavour violating doubly charged bilepton couplings contribute to the cross section via s channel resonant diagram. Therefore, it is enough to remove t and u channel contribution from the above cross section. For this case the decay width Γ_L into leptons must be enlarged.

III. INITIAL AND FINAL STATE ELECTROMAGNETIC RADIATIVE CORRECTIONS

Due to small mass of the electron, a significant role is played by the electromagnetic radiative corrections to the initial electron-positron state especially at linear collider energies. In this work we use structure function formalism

to describe the electromagnetic radiative corrections in e^+e^- colliders [18]. In the case of $e^-e^- \rightarrow \mu^-\mu^-$ process the cross section can be written in the following form within this formalism

$$\sigma(s) = \int dx_1 \int dx_2 \int dx_3 \int dx_4 D_1(x_1, s) D_2(x_2, s) D_3(x_3, s'') D_4(x_4, s'') \sigma'(s') \quad (14)$$

where $\sigma'(s')$ is the cross section with reduced energy $s' = x_1 x_2 s$. $D_1(x_1, s)$ and $D_2(x_2, s)$ stand for the initial electron structure function giving the probability of finding an electron within an electron with longitudinal momentum fractions x_1 and x_2 . $D_3(x_3, s'')$ and $D_4(x_4, s'')$ represent structure functions for the final leptons with longitudinal momentum fractions x_3 and x_4 . Here s'' is defined as $s'' = x_3 x_4 s'$. Although several definitions of the structure functions are present we use the following ones which are used by HERWIG(a multipurpose Monte Carlo event generator which has been extensively used at CERN LEP) [19]

$$D(x, Q^2) = \beta(1-x)^{\beta-1} g(x, Q^2) \quad (15)$$

$$g(x, Q^2) = e^{\beta(1+x/2)x/2} (1 - \beta^2 \frac{\pi^2}{12}) + y \frac{\beta^2}{8} y [(1+x)\{(1+x)^2 + 3 \log x\} - \frac{4 \log x}{1-x}] \quad (16)$$

$$y = [\beta(1-x)^{\beta-1}]^{-1}, \quad \beta = \frac{\alpha_{em}}{\pi} (\log \frac{Q^2}{M^2} - 1) \quad (17)$$

In expression β the value of Q^2 and M take the $s(s'')$ and initial(final) lepton mass depending on initial(final) state structure function.

To avoid divergency at the upper limit of the momentum fraction, $x = 1$, the cross section can be transformed into different form

$$\begin{aligned} \sigma(s) = & \int_0^{1-\epsilon} dx_1 dx_2 dx_3 dx_4 D_1(x_1, s) D_2(x_2, s) D_3(x_3, s'') D_4(x_4, s'') \sigma'(s') \\ & + \frac{1}{6} \sum_{i,j,k,\ell} \int_0^{1-\epsilon} dx_i dx_j dx_k D_i(x_i) D_j(x_j) D_k(x_k) \epsilon^{\beta_\ell} g_\ell(x_\ell) |_{x_\ell=1} \\ & + \frac{1}{4} \sum_{i,j,k,\ell} \int_0^{1-\epsilon} dx_i dx_j D_i(x_i) D_j(x_j) \epsilon^{\beta_k} \epsilon^{\beta_\ell} g_k(x_k) g_\ell(x_\ell) |_{x_k=1, x_\ell=1} \\ & + \frac{1}{6} \sum_{i,j,k,\ell} \int_0^{1-\epsilon} dx_i D_i(x_i) \epsilon^{\beta_j} \epsilon^{\beta_k} \epsilon^{\beta_\ell} g_j(x_j) g_k(x_k) g_\ell(x_\ell) |_{x_j=1, x_k=1, x_\ell=1} \\ & + \epsilon^{2\beta_1} \epsilon^{2\beta_3} g_1(x_1, s) g_2(x_2, s) g_3(x_3, s'') g_4(x_4, s'') |_{x_1=1, x_2=1, x_3=1, x_4=1} \end{aligned} \quad (18)$$

where ϵ can be taken as $10^{-9} - 10^{-12}$. In this region of ϵ the cross section changes by a factor of 0.99. If one takes smaller ϵ values, higher machine precision gives softer ϵ dependence. The subscript of β inside integrands is used to clarify the difference between initial and final state β values where $\beta_1 = \beta_2$ stand for initial and $\beta_3 = \beta_4$ for final leptons. The following transformation gives relatively smooth integrand

$$\begin{aligned} & \int_{x_{10}}^{1-\epsilon} dx_1 \int_{x_{20}}^{1-\epsilon} dx_2 \int_{x_{30}}^{1-\epsilon} dx_3 \int_{x_{40}}^{1-\epsilon} dx_4 D_1(x_1, s) D_2(x_2, s) D_3(x_3, s'') D_4(x_4, s'') \sigma'(s') = \\ & \int_{E_{1min}}^{E_{1max}} dE_1 \int_{F_{1min}}^{F_{1max}} dF_1 \int_{E_{2min}}^{E_{2max}} dE_2 \int_{F_{2min}}^{F_{2max}} dF_2 g_1(x_1, s) g_2(x_2, s) g_3(x_3, s'') g_4(x_4, s'') \sigma'(s') \end{aligned} \quad (19)$$

where

$$\begin{aligned} x_{10} &= \frac{\tau_{min}}{(1-\epsilon)^3}, \quad x_{20} = \frac{\tau_{min}}{x_1(1-\epsilon)^2}, \\ x_{30} &= \frac{\tau_{min}}{x_1 x_2 (1-\epsilon)}, \quad x_{40} = \frac{\tau_{min}}{x_1 x_2 x_3} \end{aligned} \quad (20)$$

$$\begin{aligned}
x_1 &= 1 - (-E_1)^{1/\beta_1} , \quad E_{1min} = -(1 - x_{10})^{\beta_1} , \quad E_{1max} = -\epsilon^{\beta_1} \\
x_2 &= 1 - (-F_1)^{1/\beta_2} , \quad F_{1min} = -(1 - x_{20})^{\beta_2} , \quad F_{1max} = -\epsilon^{\beta_2} \\
x_3 &= 1 - (-E_2)^{1/\beta_3} , \quad E_{2min} = -(1 - x_{30})^{\beta_3} , \quad E_{2max} = -\epsilon^{\beta_3} \\
x_4 &= 1 - (-F_2)^{1/\beta_4} , \quad F_{2min} = -(1 - x_{40})^{\beta_4} , \quad F_{2max} = -\epsilon^{\beta_4}
\end{aligned} \tag{21}$$

The parameter τ_{min} is a square of minimum energy fraction carried by final state leptons. Although it depends on the experimental conditions it can be taken as $\tau_{min} = 4M_f^2/s$ for theoretical purpose.

In the case of $e^-e^- \rightarrow e^-e^-$ scattering the difficulty arises due to presence of t-channel Standard Model processes. This is the two scale problem. The difficulty can be handled by the following idea. The s-channel is dominant only around the bilepton resonance region, whereas the one photon t-channel exchange dominates the cross section away from resonance region. Moreover, at large scattering angles the scale t becomes of the same order as scale s . Therefore, in the region of resonance at large angles, $e^-e^- \rightarrow e^-e^-$ scattering can be considered as one scale problem and the above calculation for initial and final state QED radiative correction is applicable in both cases.

IV. SMEARED CROSS SECTION AND DISCUSSION

In order to account for a finite resolution in the invariant mass of final state leptons $M_{\ell\ell}$, we consider a smeared cross section as defined below

$$\sigma(s_0) = \int_{E_0-D/2}^{E_0+D/2} \frac{dE}{\sqrt{2\pi}D} \exp\left[-\frac{(E_0 - E)^2}{2D^2}\right] \sigma(s) \tag{22}$$

where $E_0 = \sqrt{s_0}$ and $E = \sqrt{s}$. Smearing parameter D corresponds to an overall energy resolution. The effect of ISR, FSR and smearing can be seen from Table I which shows the significance

$$S = \frac{|\sigma - \sigma_{SM}|}{\sqrt{\sigma_{SM}}} \sqrt{L_{int}} \tag{23}$$

for the process $e^-e^- \rightarrow e^-e^-$ at a resonance point with an assumed bilepton mass $M_L = 500$ GeV and an integrated luminosity $L_{int} = 10000 pb^{-1}$. In previous works, indirect upper limits on the bilepton-lepton-lepton couplings were found to be of the order of $O(10^{-1})$ using CERN LEP data for the bilepton masses 200-800 GeV [13, 14]. For comparison we take three values of coupling $g_L = 0.1, 0.01, 0.001$ and two values of the smearing parameter $D=0.05, 5$ GeV. Depending on the couplings and bilepton mass, the values of the bilepton decay width to leptons are also exhibited in the table to compare with D parameter. It is clear from the values of the significance S_0 that the cross section is independent of the coupling at the resonance point when ISR, FSR and smearing are not included. Since we consider only lepton decay channels of bileptons the decay width is very narrow for small couplings and for the masses specified above. Therefore, there is a difficulty to observe invariant masses of two leptons $M_{\ell\ell}$ experimentally. If the experimental energy resolution is around $D=0.01E$ ($D=5$ GeV) the decay width is $\Gamma_L \ll D$ and the significance drastically reduces due to ISR, FSR and smearing. Moreover, for the coupling $g_L = 0.001$ the peak is unobservable because of $S_2 \ll 1$. If we assume higher energy resolution such as $D=0.0001E$ ($D=0.05$ GeV) the bilepton decay width $\Gamma_L > D$ for only $g_L = 0.1$ and there is no need to consider smeared cross section. However, for smaller couplings S_2 needs to be considered. In this case, the bileptons can be observed also for the coupling $g_L = 0.001$.

Similar features are shown in Fig. 1 for the resonance in $e^-e^- \rightarrow \mu^-\mu^-$ process at a resonance point $E_{cm} = M_L = 800$ GeV with the smearing parameter $D = 0.0001E$. Here we assume lepton flavour number is violated. The bilepton-lepton-lepton coupling $g_L = 0.01$ and $\tau_{min} = 0.01$ are taken into account. The cross section at the peak of the resonance is about 200pb without ISR, FSR and smearing. ISR and FSR reduce the cross section to 46pb whereas the smearing in addition to ISR+FSR reduces it to 4pb, i.e. almost 50 times smaller than the highest point. If we consider lepton flavour is conserved the resonance peak should be observed in the process $e^-e^- \rightarrow e^-e^-$ with the SM background of Moeller scattering. In addition to $g_L = 0.01$ and $\tau_{min} = 0.01$ we apply a cut on the scattering angle $|\cos\theta| = 0.8$ to avoid t-channel instabilities. In this case, bilepton decay width to leptons is highly narrower than the case of lepton flavour violation. More clearly, Fig. 2 shows this behaviour of cross sections at an assumed resonance point ($M_L = 800$ GeV) with and without ISR+FSR and smearing including Standard Model background (Moeller scattering). With a smearing parameter $D > 0.0001E$ the peak in the invariant mass of M_{ee} is hardly observable

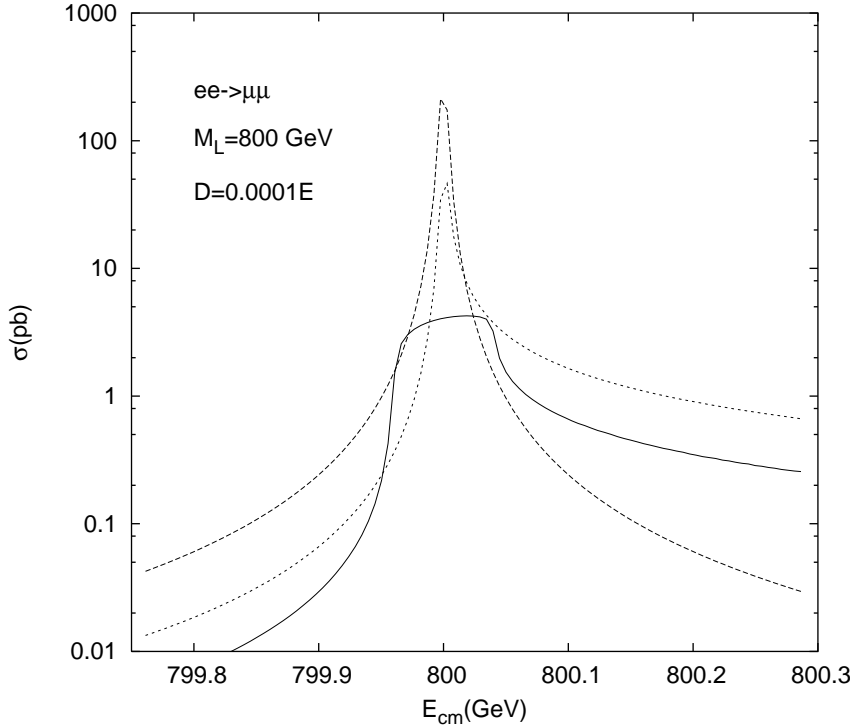


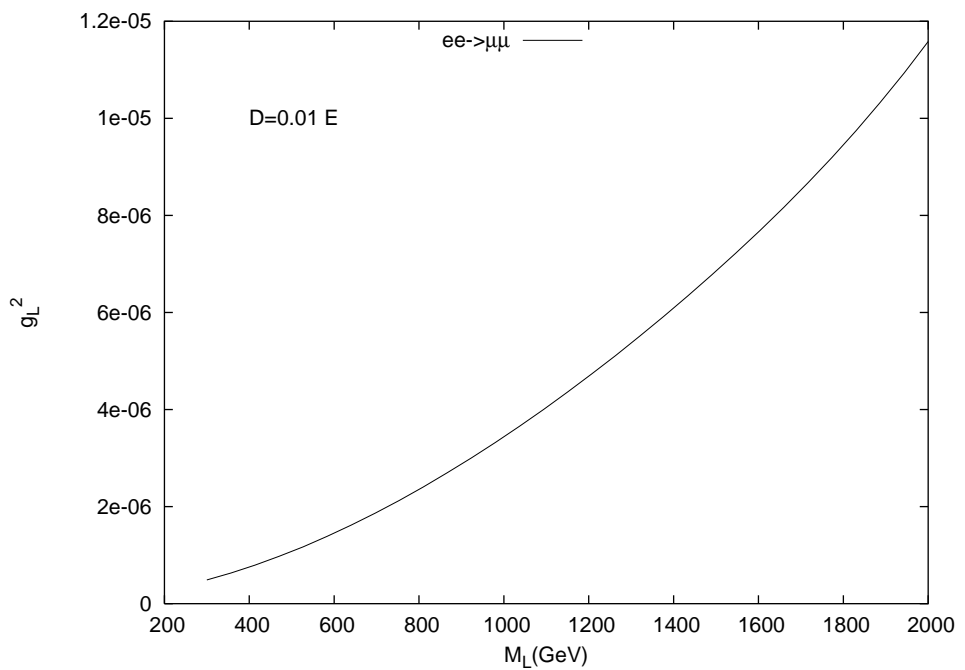
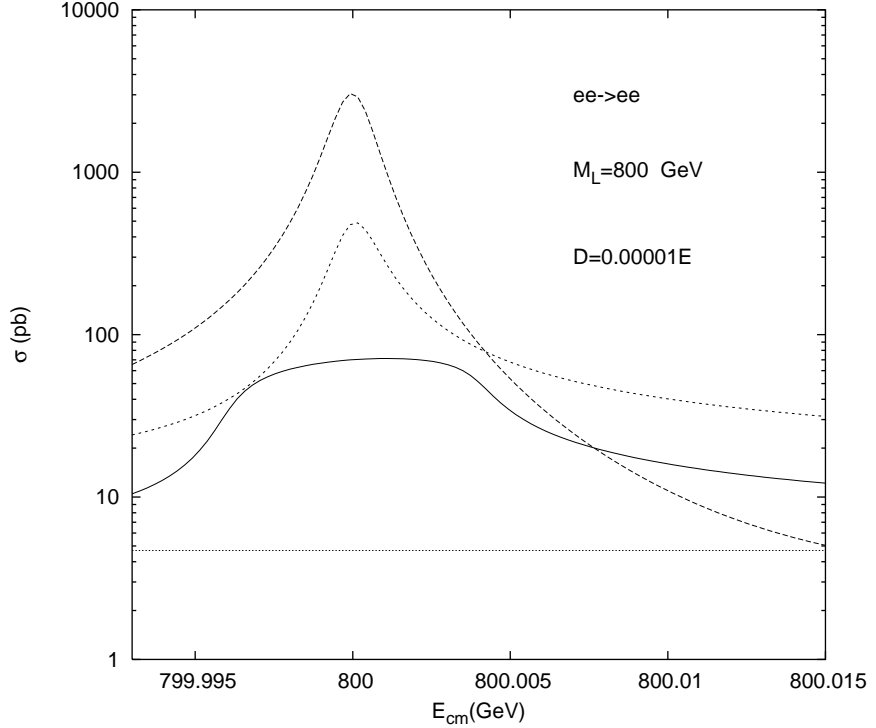
FIG. 1: Bilepton resonance curves from the process $e^-e^- \rightarrow \mu^-\mu^-$ assuming bilepton mass is $M_L = 800$ GeV. The highest curve around the resonance point is free of initial, final state radiative corrections(ISR, FSR) and smearing effect on the cross section. The second curve includes ISR and FSR. The lowest curve covers ISR, FSR and smearing effect with smearing parameter $D=0.0001E$.

TABLE I: Comparison of the significances S_0 , S_1 and S_2 for the process $e^-e^- \rightarrow e^-e^-$ at an assumed resonance point $M_L = 500$ GeV to demonstrate the influence of the initial, final state electromagnetic radiative corrections and smearing effect. S_1 is the significance with ISR+FSR and S_2 with ISR+FSR and smearing. S_0 does not cover any corrections and smearing.

g_L	$D(\text{GeV})$	$\Gamma_L(\text{GeV})$	S_1	S_2	S_0
0.1	5	0.1	40000	1400	200900
0.01	5	0.001	19800	10	200900
0.001	5	0.00001	9700	0.04	200900
0.1	0.05	0.1	40000	-	200900
0.01	0.05	0.001	19800	700	200900
0.001	0.05	0.00001	9700	5	200900

after smearing due to SM background. For illustration we use $D=0.00001E$ in Fig. 2. Therefore, we will need high resolution detectors to discover bileptons from this process.

In order to estimate discovery contour of g_L^2 and M_L we use one parameter one sided χ^2 analysis at %95 C.L. and 5σ significance for $e^-e^- \rightarrow e^-e^-$ process. In the case of lepton flavour violating process $e^-e^- \rightarrow \mu^-\mu^-$ there is no SM background and all the events consist of signal events. Then, %95 C.L. contour can be obtained by taking Poisson variable as the observed events with Poisson mean $\nu = 9.15$. In Fig. 3 and Fig. 4 discovery contour of g_L^2 and M_L are plotted from the lepton flavour violating process including ISR+FSR and smearing with smearing parameter $D=0.01E$ and $D=0.0001E$. Fig. 5 shows the similar curves for the lepton flavour conserving process with $D=0.0001E$. In all these figures the left part of the each curve is the allowed region. Certainly, higher luminosity creates more allowed region.



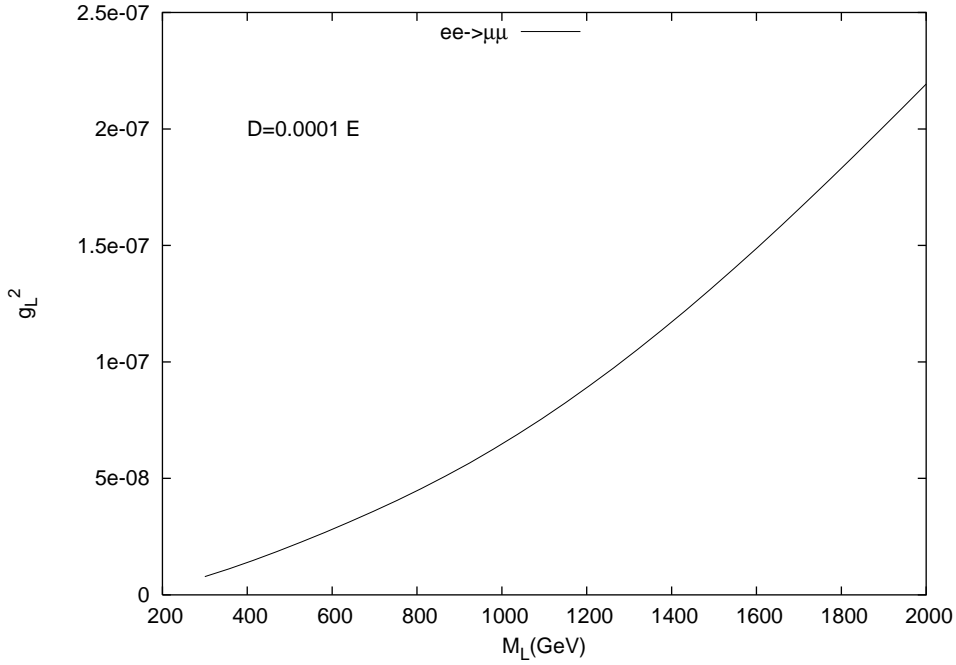


FIG. 4: The same as the previous figure but for the smearing parameter $D=0.0001E$.

[1] Y. Fukuda et al., Super-Kamiokande Collaboration, *Phys. Lett. B* **433**(1998)9; *Phys. Lett. B* **436**(1998)33; *Phys. Rev. Lett.* **81**(1998)1562; J.N. Bahcall et al., *Nucl. Phys. Proc. Suppl.* **100**(2001)5; SNO Collaboration, *nucl-ex/0106015*.

[2] T.G. Rizzo, *Phys. Rev. D* **25**(1982)1355; J.F. Gunion, H.E. Haber, G. Kane, S. Dawson *The Higgs Hunters Guide*, Addison-Wesley (1990); K. Huitu and J. Maalampi, *Phys. Lett. B* **344** (1995)217.

[3] R. Barbieri, L. Hall and A. Strumia, *Nucl. Phys. B* **445**(1995)219; Y. Okada, KEK-TH-606, *hep-ph/9811502*.

[4] R.N. Mohapatra, G. Senjanovic, *Phys. Rev. Lett.* **44**(1980)14; R.N. Mohapatra, G. Senjanovic, *Phys. Rev. D* **23**(1981)165.

[5] P.H. Frampton, *Int. J. Mod. Phys. A* **13** (1998)2345.

[6] G.G. Ross, *Grand Unified Theories*, Benjamin-Cummins (1985); E. Fahri, L. Suskind *Phys. Rep.* **74** (1981) 277; E. Eichten et al., *Rev. Mod. Phys.* **56** (1984)579; W. Buchmüller, *Acta Phys. Austr. Suppl.* XXVII (1985)517.

[7] T. Rizzo, *Phys. Rev. D* **27** (1983)657; N. Lepore, B. Thorndyke, H. Nadeau and D. London, *Phys. Rev. D* **50**(1994)2031; G. Barenboim, K. Huitu, J. Maalampi and M. Raidal, *Phys. Lett. B* **394** (1997)132; J.F. Gunion, *Int. J. Mod. Phys. A* **13** (1998)2277.

[8] F. Cuypers and S. Davidson, *Eur. Phys. Jour. C* **2** (1998)503.

[9] M.L. Swartz, *Phys. Rev. D* **40** (1989)1521.

[10] H. Fujii, Y. Mimura, K. Sasaki and T. Sasaki, *Phys. Rev. D* **49** (1994)559.

[11] D. Chang and W. -Y. Keung, *Phys. Rev. Lett.* **62** (1989)2583.

[12] L. Willmann et al., *Phys. Rev. Lett.* **82** (1999) 49.

[13] S. Atag and K.O. Ozansoy, *Phys. Rev. D* **68** (2003) 093008; S. Atag and K.O. Ozansoy, *Phys. Rev. D* **70** (2004) 053001;

[14] OPAL Collaboration, G. Abbiendi et al., *Phys. Lett. B* **577**(2003)93.

[15] DELPHI Collaboration, J. Abdallah et al., *Phys. Lett. B* **552**(2003)127.

[16] J.F. Gunion, *Int. J. Mod. Phys. A* **11**(1996)1551; F. Cuypers and M. Raidal, *Nucl. Phys. B* **501** (1997)3.

[17] Information about the latest status of the future linear colliders can be found at:
<http://www.interactions.org/linearcollider>.

[18] E.A. Kuraev, V.S. Fadin, *Sov. J. Nucl. Phys.* **41**, 466 (1985);
 G. Alterelli, G. Martinelli, in *Physics at LEP*, J. Ellis, R. Peccei eds. CERN 86-02 (CERN, Geneva, 1986);
 O. Niclosini, L. Trentadue, *Phys. Lett. B* **196**, 551 (1987); Z. Phys. **C39**, 479 (1988);
 F.A. Berends, G. Burgers, W.L. van Neerven, *Nucl. Phys. B* **297**, 429 (1988).

[19] G. Alterelli, T. Sjostrand and F. Zwirner eds., *Physics at LEP2*, vol.2 p139, CERN yellow report 96-01.

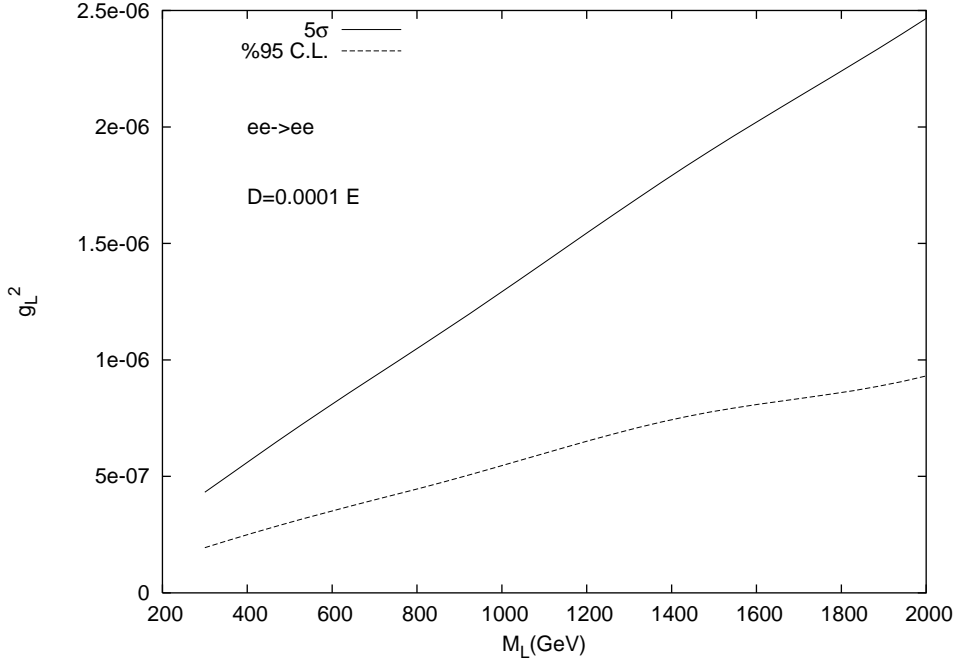


FIG. 5: 5σ and $\%95$ C.L. contour of the bilepton-lepton-lepton coupling squared g_L^2 and bilepton mass M_L coming from lepton flavour conserving $e^-e^- \rightarrow e^-e^-$ scattering. Each curve has been obtained by considering ISR, FSR and smeared cross section with smearing parameter $D=0.0001E$. The left part of the each curve is the allowed region.